

Simulation and calculation of internal faults in long-stator linear synchronous motor based on winding function theory

Yu Fang Yu Haitao Hu Minqiang

(School of Electrical Engineering, Southeast University, Nanjing 210096, China)

Abstract: To guarantee the safety of the high speed maglev train system, a novel model based on the winding function theory is proposed for the long-stator linear synchronous motor (LSM), which is suitable for the real-time calculation of the running state. The accurate coupled mathematical models under different internal fault conditions of the LSM are derived based on the normal model. Then the fault currents and electromagnetic forces are simulated and calculated for the major potential internal faults of the LSM, such as the single-phase short circuit, the phase-phase short circuit and the single-phase open circuit. The characteristic curve between the electromagnetic force and the armature current of the LSM, which is compared with the results from the finite element method, proves the validation of the proposed method. The fault rule is determined and the proposed analytical model also shows its feasibility in the fast fault diagnosis through the comparison of the simulation results of currents and electromagnetic forces under different internal fault types and short circuit ratios.

Key words: long-stator linear synchronous motor; winding function theory; internal faults

With the rapid development of the social economy, the increasing demand for mass transportation systems has emerged. The high-speed maglev train system is a new transportation system which first appeared in Shanghai for commercial use in 2003. The advantages over its high speed, low noise and non-pollution make it suitable for long distance transportation compared with the conventional wheel-on-rail train system. However, the internal faults of the long-stator linear synchronous motor (LSM) can cause serious consequences to the passengers on the trains. So, quickly simulating and calculating the faults of the LSM becomes very important to prevent extensive failure and make preparations for further fault detection and diagnosis.

For the purpose of accurately modeling and simulating for the LSM, an appropriate mathematic model should be established. Although the traditional dq0 model is usually introduced for simulating synchronous motors, it is not suitable for stator internal fault modeling, as the symmetry between the stator windings no longer exists. A novel method based on the winding function theory^[1-3] is presented in this paper for the accurate calculation of inductances under normal and faulty windings of the LSM model. In fact, according to this approach, it is possible to compute all kinds of ma-

chines having normal or asymmetric windings, while taking into account all of the spatial harmonic components. The corresponding voltage and flux linkage equations of the system can then be derived after the impedance matrix has been calculated. In recent years, this method has been successfully used to analyze the air-gap eccentricity of the salient-pole motor and the cage induction motor^[4-6].

The potential internal stator faults of the LSM generally contain a single-phase open circuit, a phase-phase short circuit and a single-phase short circuit, etc., any of which can cause severe damage to the train system. Therefore, fast diagnosis and detection for the LSM is very necessary to prevent extensive failure. Accurate calculation of the electromagnetic forces is just the key to further fault diagnosis^[7-9], as the electromagnetic forces contain more interactions between stator-mover flux linkage and seem to be more sensitive to internal faults compared with the single current signal. The faulty symptoms, when a long-stator linear synchronous motor incurs some kind of internal faults, are gained through the comparison of the simulation results of electromagnetic forces under different internal fault conditions, which can be used for later internal fault diagnosis and fast recognition^[10].

1 Modeling for LSM

1.1 Working principle of LSM

The stator part of the long-stator LSM is the guide-way lying on the ground^[11], which is supplied with the three-phase alternating current, and the vehicle is regarded as the mover part which is equipped with levitation magnets supplied by the direct current. The interaction of the magnetic fields caused by the stator currents and the excitation current achieves the linear motion and stable levitation of the maglev train. As the number of slots per pole is an integer in this LSM model and the rotor has a symmetrical structure, it is adequate for simulating the two poles model of the LSM. Fig. 1 shows the longitudinal section of the LSM model in one polar pitch.

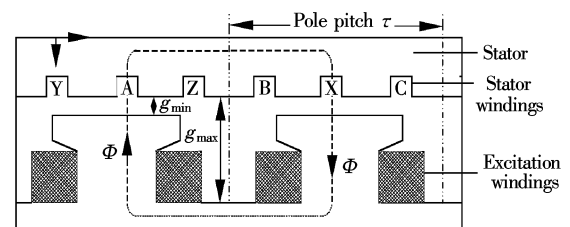


Fig. 1 Longitudinal section of the LSM model

The essential parameters of the LSM model for impedance calculation are shown in Tab. 1.

Received 2009-07-22.

Biographies: Yu Fang (1985—), female, graduate; Yu Haitao (corresponding author), male, doctor, professor, htyu@seu.edu.cn.

Citation: Yu Fang, Yu Haitao, Hu Minqiang. Simulation and calculation of internal faults in long-stator linear synchronous motor based on winding function theory [J]. Journal of Southeast University (English Edition), 2010, 26(1): 53 – 57.

Tab. 1 LSM parameters

Parameter	Value
Number of poles	2
Pole pitch/mm	258
Stator slot height/mm	43
Stator slot width/mm	43
Air-gap/mm	10
Number of stator turns	1
Number of excitation turns	270

1.2 Winding function theory in LSM

In a conventional rotational machine, the mutual inductance of two armature windings a and b can be written by the winding function as follows^[1-4], which can take into account all space harmonics and apply to the calculation of the inductance matrix under normal and fault conditions,

$$L_{ab} = \mu_0 r l \int_0^{2\pi} g^{-1}(\phi, \theta) N_a(\phi, \theta) N_b(\phi, \theta) d\phi \quad (1)$$

where $g^{-1}(\phi, \theta)$ is the inverse air-gap length function, and $N(\phi, \theta)$ is the winding function of the stator or the rotor phase. In the case of the LSM, Eq. (1) should be modified, as the winding function of the LSM is not the function of the rotor angle anymore but the function of the relative position of the mover. It can be expressed as $N(x, x')$, which is the function of displacement of the stator and the mover. It is usually assumed that the circuits of the phases are approximated as sinusoidally distributed. The inverse air-gap function should also be modified accordingly. Take the calculation of the mutual inductance of stator phase a and excitation phase f for example,

$$M_{af} = \mu_0 w \int_0^{2\tau} N_a(x, x') N_f(x, x') g^{-1}(x, x') dx = L_{af0} \cos\left(\frac{\pi}{\tau} x\right) \quad (2)$$

$$g^{-1}(x, x') = \alpha_0 - \alpha_2 \cos\left(\frac{2p\pi}{\tau}(x - x')\right) \quad (3)$$

where M_{af} is the mutual inductance between phase a and excitation phase f; $g^{-1}(x, x')$ is the inverse air-gap function; p is the number of the pole pairs.

The inverse air-gap function is described in the form of Eq. (3), because the magnetic circuit of the machine is symmetrically distributed from each polar of the motor. The inverse air-gap function only has even-order harmonic components and the higher components are ignored. The waveforms of the mutual inductances among phases a, b, c and f are given in Fig. 2, from which it can be seen that the mutual inductance is a varying value with the position of the mover.

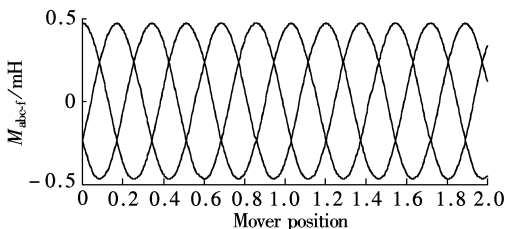


Fig. 2 Mutual inductances among phases a, b, c and excitation winding f

1.3 Mathematical model of LSM

After the impedance matrix has been accurately calculated, the exact coupled mathematical model for the LSM is formed. Some appropriate simplifications should be taken into account first, such as ignoring the effects of iron saturation and magnetic hysteresis.

It is convenient to describe the idealized LSM model as three-phase stator windings and an excitation winding. The system equation under normal conditions can be written as

$$\begin{bmatrix} L_{ss} & L_{sf} \\ L_{fs} & L_f \end{bmatrix} \begin{bmatrix} \frac{dI_{ss}}{dt} \\ \frac{dI_f}{dt} \end{bmatrix} = \begin{bmatrix} u_{ss} \\ u_f \end{bmatrix} - \begin{bmatrix} r_s + v \frac{dL_{ss}}{dx} & v \frac{dL_{sf}}{dx} \\ v \frac{dL_{fs}}{dx} & r_f + v \frac{dL_f}{dx} \end{bmatrix} \begin{bmatrix} I_{ss} \\ I_f \end{bmatrix} \quad (4)$$

$$L_{ss} = \begin{bmatrix} L_{aa} & M_{ab} & M_{ac} \\ M_{ab} & L_{bc} & M_{bc} \\ M_{ac} & M_{bc} & L_{cc} \end{bmatrix}, \quad L_{sf} = \begin{bmatrix} M_{af} \\ M_{bf} \\ M_{cf} \end{bmatrix} \quad (5)$$

$$L_{sf} = L_{fs}^T \quad (6)$$

$$\frac{dI}{dt} = - \left[L^{-1} \left(r + \frac{dL}{dt} \right) \right] I + L^{-1} U \quad (7)$$

Substituting the impedance matrix into Eq. (1), the current differential Eq. (7) can be solved by using an appropriate numerical integration method, and, hence, the current vector I can be obtained. Since the elements of the inductance matrix are the function of the displacement x of the mover, they are time variant. The propulsion and levitation forces, thereupon, can also be obtained, which are very important in analyzing the operational performance of the maglev train. In the case of the stator faults, the impedance matrix is recalculated and the mathematical model is accordingly changed.

2 Simulation Results under Different Conditions

As the calculation of the electromagnetic forces is the key to the model for the LSM, an accurate analytical formula derived from the whole machine energy is proposed and applied in this paper. Unlike the rotating machine, the electromagnetic forces of the LSM can be divided into two parts, the propulsion force, which is used for driving the vehicle going ahead, and the levitation force, which guarantees the steady levitation of the vehicle. These forces under different running conditions are analyzed in the following.

2.1 Results under normal condition

The simulation waveforms of the currents and electromagnetic forces under the normal condition of the LSM are shown in Fig. 3, where the power angle of the system stays at 90° .

From the waveforms of Fig. 3, it can be seen that when the speed and the power angle of the maglev train system keep constant and the effect of stator slot is ignored, the currents and electromagnetic forces all hold in steady-state and the value of the levitation force is several times that of the propulsion force.

The control system of the LSM achieves the decoupling

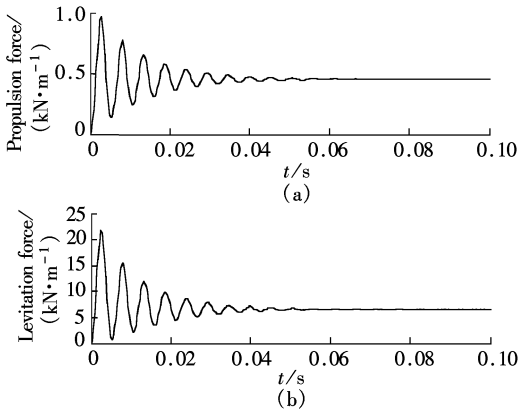


Fig. 3 Electromagnetic forces of the LSM under normal condition. (a) Propulsion force; (b) Levitation force

control of the propulsion and levitation forces. That is to say, a stable levitation force is guaranteed by controlling the levitation excitation current and the propulsion force is mainly related to the stator currents when the excitation current keeps the same.

Fig. 4 gives the relationship between the height of the air-gap and the electromagnetic forces. It can be regarded as the electromagnetic forces declining with the increment in the air-gap. When the air-gap is greater than 8 mm, the rate of the electromagnetic forces decreases relatively slower; therefore, it can be considered that the greater the height of the air-gap is, the easier it is for us to control the train system. The levitation gap in this model is controlled to be 10 mm.

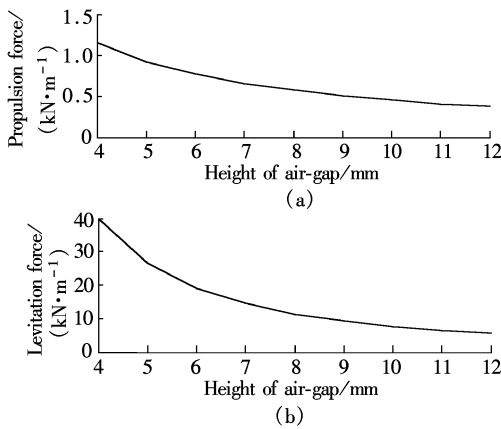


Fig. 4 Relationship between electromagnetic forces and the air-gap height. (a) Propulsion force; (b) Levitation force

2.2 Results under single-phase short circuit

There are three kinds of internal faults discussed in this paper, a single-phase short circuit, a phase-phase short circuit and a single-phase open circuit. Once any kind of these faults occurs, it will cause serious consequences to the safety operation of the long-stator LSM system. Hence, the simulation and calculation of these fault conditions is necessary and useful for further fault diagnosis.

Suppose that in phase a, a single-phase short circuit occurs. The faulty winding is separated into two parts by the short circuit ratio k , and then the corresponding impedance matrix and voltage equation are modified and recalculated accordingly.

$$\begin{bmatrix} L'_{ss} & L'_{sf} \\ L'_{fs} & L'_{ff} \end{bmatrix} \begin{bmatrix} \frac{dI_{ss}}{dt} \\ \frac{dI_{ff}}{dt} \end{bmatrix} = \begin{bmatrix} u'_{ss} \\ u'_{ff} \end{bmatrix} - \begin{bmatrix} r'_s + v \frac{dL'_{ss}}{dx} & v \frac{dL'_{sf}}{dx} \\ v \frac{dL'_{fs}}{dx} & r'_f + v \frac{dL'_{ff}}{dx} \end{bmatrix} \begin{bmatrix} I_{ss} \\ I_{ff} \end{bmatrix} \quad (8)$$

$$L'_{ss} = \begin{bmatrix} L_{a11} & M_{a12} & M_{a1b} & M_{a1c} \\ M_{a21} & L_{22} & M_{a2b} & M_{a1c} \\ M_{ba1} & M_{ba2} & L_{bb} & M_{a1c} \\ M_{ca1} & M_{ca2} & M_{cb} & L_{cc} \end{bmatrix}, \quad [L'_{sf}] = \begin{bmatrix} M_{a1f} \\ M_{a2f} \\ M_{bf} \\ M_{cf} \end{bmatrix} \quad (9)$$

$$L'_{sf} = L'_{fs}^T \quad (10)$$

where

$$r' = \begin{bmatrix} r'_s & \\ & r'_f \end{bmatrix} = \text{diag}[(1-k) \quad k \quad 1 \quad 1 \quad 1] \times \text{diag}[r \quad r \quad r \quad r \quad r] \quad (11)$$

$$L_{a11} = (1-k)L_{1s} + (1-k)^2 L_{am} \quad (12)$$

$$L_{a22} = kL_{1s} + k^2 L_{am} \quad (13)$$

The other parameters of the inductance matrix can be recalculated with the same method using Eqs. (12) and (13), and the relative simulation results are given in Fig. 5 and Fig. 6.

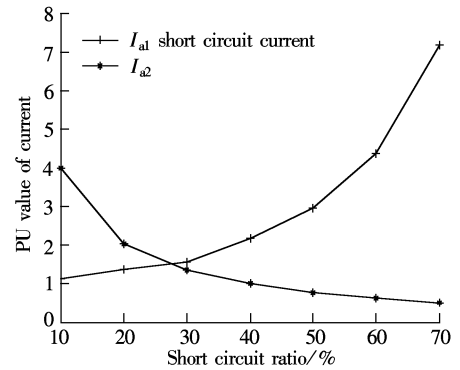


Fig. 5 The PU value of short circuit current under different short circuit ratios of phase a

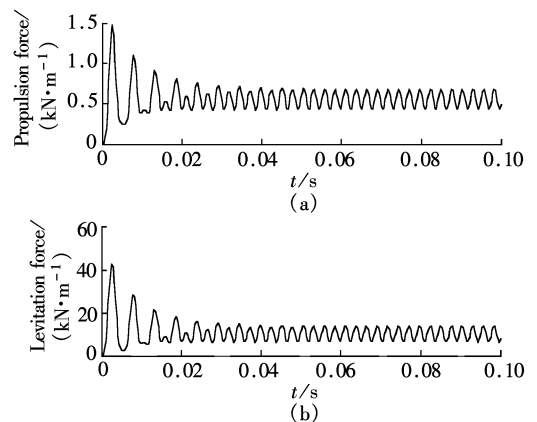


Fig. 6 Electromagnetic forces under 30% single phase short circuit. (a) Propulsion force; (b) Levitation force

The short circuit current of phase a changes with the increment of short circuit ratios as shown in Fig. 5. Whatever

kinds of internal faults occur, the electromagnetic forces of the machine cannot maintain a stable value and the harmonic components also strengthen, as shown in Fig. 6, when the single-phase short circuit occurs in phase a.

2.3 Phase-phase short circuit and single-phase open circuit

A similar analytical technique is used to build the models when the phase-phase short circuit or single-phase open circuit occurs. Here only some simulation results are given. Fig. 7 shows the propulsion forces of the phase-phase short circuit and the single-phase open circuit. The oscillation amplitudes are different when different faults occur. It also means that the harmonic components contained in each faulty waveform are different, which is the basis for fault diagnosis.

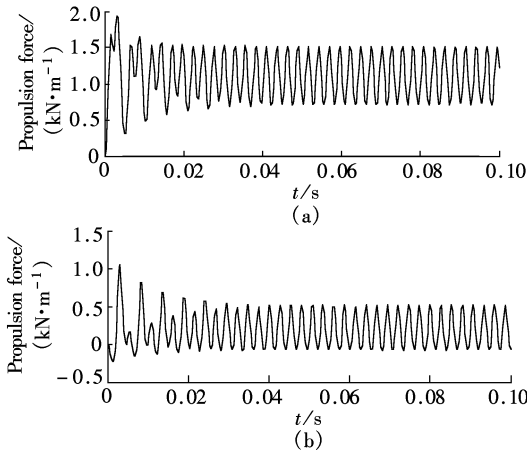


Fig. 7 Propulsion force. (a) Under 50% phase-phase short circuit; (b) Under single-phase open circuit

In fact, the amplitude value of the currents and electromagnetic forces also enlarges with varying degrees of fault type, which is in accordance with the theoretical trend of the rotating machine. As a result, the simulation currents validate the usability of the model proposed in this paper.

3 Comparison of Results

In order to verify the analytical formulae applied in calculating the electromagnetic forces, a finite element 2D model using the same geometric parameters is set up. Through the comparison of characteristic curves of the two methods, it can be obtained that the analytical formulae are reliable and convenient. The power-angle curve shows that the propulsion force grows with the increment in the power-angle when it is less than 90° . On the contrary, when the power-angle is greater than 90° , the propulsion force declines with the increment. Similarly, the levitation force decreases with the increment of the power-angle. Fig. 8 shows the relationship between the armature current and the propulsion force.

There must appear some fault symptoms when some kinds of stator internal faults occur. Therefore, it is urgent to determine the exact fault symptoms to identify the fault type. In further work, some fault diagnosis methods such as the expert system and the neural network can be used for dealing with the electromagnetic forces to determine appropriate fault eigenvectors of the LSM.

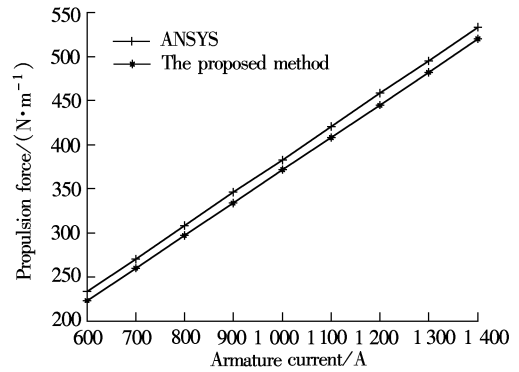


Fig. 8 Relationship between propulsion force and armature current

4 Conclusion

A new mathematical model is established for the long-stator linear synchronous motor based on the winding function theory, which makes the calculation of the impedance parameters more simple and more accurate. The electromagnetic forces under different internal faults of the LSM, which contain many fault symptoms, are then simulated and analyzed by the proposed method. According to the simulation results, the proposed method is proved to be useful in fault diagnosis and can be developed as an effective protection method for the LSM.

References

- [1] Tu Xiaoping, Dessaint L-A, Fallati N, et al. Modeling and real-time simulation of internal faults in synchronous generators with parallel-connected windings [J]. *IEEE Transactions on Industrial Electronics*, 2007, **54**(3): 1400–1409.
- [2] Toliyat H A, Al-Nuaim N A. Simulation and detection of dynamic air-gap eccentricity in salient-pole synchronous machines [J]. *IEEE Transactions on Industry Applications*, 1999, **35**(1): 86–93.
- [3] Tabatabaei I, Faiz J, Lesani H, et al. Modeling and simulation of a salient-pole synchronous generator with dynamic eccentricity using modified winding function theory [J]. *IEEE Transactions on Magnetics*, 2004, **40**(3): 1550–1555.
- [4] Toliyat H A, Lipo T A. Transient analysis of cage induction machine under stator, rotor bar and end ring fault [J]. *IEEE Transactions on Energy Conversion*, 1995, **10**(2): 241–247.
- [5] Faiz J, Tabatabaei I. Extension of winding function theory for nonuniform air gap in electric machinery. [J]. *IEEE Transactions on Magnetics*, 2002, **38**(6): 3654–3657.
- [6] Megahed A I, Malik O P. Simulation of internal faults in synchronous generators [J]. *IEEE Transactions on Energy Conversion*, 1999, **14**(4): 1306–1311.
- [7] Andriollo M, Martinelli G, Morini A, et al. FEM calculation of the LSM propulsion force in EMS-MAGLEV trains [J]. *IEEE Transactions on Magnetics*, 1996, **32**(5): 5064–5066.
- [8] Andriollo M, Martinelli G, Morini A, et al. Electromagnetic optimization of EMS-MAGLEV systems [J]. *IEEE Transactions on Magnetics*, 1998, **34**(4): 2090–2092.
- [9] Coulomb J L, Meunier G. Finite element implementation of virtual work principle for magnetic or electric force and torque computation [J]. *IEEE Transactions on Magnetics*, 1984, **20**(5): 1894–1896.

- [10] Kerezi B, Howard I. Vibration fault detection of large turbogenerators using neural networks [C]//*Proceedings of IEEE International Conference on Neural Networks*. Perth, WA, Australia, 1995: 121 - 126.
- [11] Ye Yunyue. *The theory and application of linear machines* [M]. Beijing: China Machine Press, 2000. (in Chinese)

基于绕组函数理论的长定子直线同步电机内部故障仿真计算

于芳 余海涛 胡敏强

(东南大学电气工程学院, 南京 210096)

摘要: 为了保证高速磁浮列车系统安全牵引运行, 提出一种基于绕组函数理论的新颖模型并用该模型对长定子直线同步电机进行建模, 便于实时计算列车的运行状态. 首先在正常运行模型的基础上推导长定子直线同步电机在不同故障状态下的精确耦合数学模型, 然后对其运行时存在的主要潜在定子绕组内部故障如单相短路、相间短路和单相开路等进行故障电流、电磁力仿真计算. 将计算得到的直线电机运行电磁力随定子电流变化的特性曲线与有限元方法的结果进行对比, 验证了所提出的电磁力公式的准确性. 通过比较在不同故障类型和故障短路比下故障电流、电磁力仿真结果的变化情况, 找出了内部故障规律, 同时显示了此解析数学模型在电机故障快速识别中具有可用性.

关键词: 长定子直线同步电机; 绕组函数理论; 内部故障

中图分类号: TM341